A New Generation of Peptide-based Inhibitors Targeting HIV-1 Reverse Transcriptase Conformational Flexibility.

Audrey Agopian, Edwige Gros, Gudrun Aldrian-Herrada, Nathalie Bosquet, Pascal Clayette, Gilles Divita

A NEW GENERATION OF PEPTIDE-BASED INHIBITORS TARGETING HIV-1 REVERSE TRANSCRIPTASE CONFORMATIONAL FLEXIBILITY.

Audrey Agopian[1], Edwige Gros[1], Gudrun Aldrian-Herrada[1], Nathalie Bosquet[2], Pascal Clayette[2] & Gilles Divita[1*]

[1] Centre de Recherches de Biochimie Macromoléculaire, Department of Molecular Biophysics & Therapeutic, UMR-5237 CNRS-UM2-UM1, 1919 Route de Mende, 34293 Montpellier, France
[2] SPI-BIO CEA, Pharmacologie des Rétrovirus, 18 route du panorama, BP6, 9226 Fontenay aux Roses, France.
Running title: Peptide inhibitors of HIV-1 Reverse Transcriptase conformational flexibility
* To whom correspondence should be addressed. Tel : (33) 04 67 61 33 92. Fax: (33) 04 67 52 15 59; E-mail : gilles.divita@crbm.cnrs.fr

The biologically active form of Human Immunodeficiency Virus type 1 Reverse Transcriptase (RT) is a heterodimer. The formation of RT is a two-step mechanism, including a rapid protein/protein interaction "the dimerization step", followed by conformational changes "the maturation step", yielding the biologically active form of the enzyme. We have previously proposed that the heterodimeric organization of RT constitutes an interesting target for the design of new inhibitors. Here, we propose a new class of reverse transcriptase inhibitors that targets protein/protein interactions and conformational changes involved in the maturation of heterodimeric reverse transcriptase. Based on a screen of peptides derived from the thumb domain of this enzyme, we have identified a short peptide P_{AW} that inhibits the maturation step and blocks viral replication at subnanomolar concentrations. P_{AW} only binds dimeric RT and stabilizes it in an inactive/ non processive conformation. From a mechanistic point of view, P_{AW} prevents proper binding of primer/template by affecting the structural dynamics of the thumb/fingers of p66 subunit. Taken together, these results demonstrate that HIV-1 RT maturation constitutes an attractive target for AIDS chemotherapeutics

Human immunodeficiency virus type I (HIV-1) is the primary cause of acquired immunodeficiency syndrome (AIDS), a slow progressive and degenerative disease of the human immune system. Despite recent therapeutic developments and the introduction of Highly Active Antiretroviral Therapy (HAART), the rapid emergence of drug-resistant viruses against all approved drugs together with inaccessible latent virus reservoirs and side effects of currently used compounds have limited the efficacy of existing anti-HIV-1 therapeutics (1).Therefore, there is still an urgent need for new and safer drugs, active against resistant viral strains or directed towards novel targets in the replicative cycle, which will be useful for multiple drug combination.

HIV-1 reverse transcriptase (RT) plays an essential multifunctional role in the replication of the virus, by catalysing the synthesis of double-stranded DNA from the single-strand retroviral RNA genome (2,3). The majority of the chemotherapeutic agents used in AIDS treatments target the polymerase activity of HIV-1 RT, such as nucleoside reverse transcriptase inhibitors (NRTI) or non-nucleoside inhibitors (NNRTI) (4). The biologically active form of RT is an asymmetric heterodimer that consists of two subunits, p66 and p51 derived from p66 by proteolytic cleavage of the C-terminal RNAse H domain (2,3,5).

The polymerase domain of both p66 and p51 subunit can be subdivided into four common subdomains: fingers, palm, thumb and connection (6-10). Determination of the three-dimensional structures of RTs has revealed that although the folding of individual subdomains is similar in p66 and p51, their spatial arrangement differs markedly (11). The p66 subunit contains both polymerase and RNase H active sites. The p66-polymerase domain folds into an "open", extended structure, forming a large active site cleft with the three catalytic residues (Asp^{110}, Asp^{185}, Asp^{186}) within the palm subdomain exposed in the nucleic acid binding site. The primer grip is responsible for the appropriate placement of the primer terminus at the

polymerase active site and is involved in translocation of the primer-template (p/t) following nucleotide incorporation (12-14). In contrast, p51 predominantly plays a structural role in the RT heterodimer, by stabilizing the dimer interface thereby favouring loading of the p66 onto the p/t and maintaining the appropriate enzyme conformation during initiation of reverse transcription (15).

In order to propose new classes of HIV inhibitors, extensive efforts have been made in the design of molecules that target protein/protein interfaces required for viral entry, replication and maturation (16-19). We (20,22) and others (5,24) have proposed that the heterodimeric organization of RT constitutes an interesting target for the design of new inhibitors. The formation of the active heterodimeric HIV-1 RT occurs in a two step process. First a rapid association of the two subunits (dimerization-step) via their connection sub-domains thereby yielding an inactive intermediate-RT, followed by a slow conformational change of this intermediate (maturation-step), generating the biologically active form of this enzyme. The maturation step involves contacts between the thumb of p51 and the RNAse H of p66 as well as between the fingers of p51 with the palm of p66 (20-23). NNRTIs have been reported to interfere with RT dimerization and to modulate the overall stability of the heterodimeric RT depending on their binding site on RT (24-28). NNRTIs including Efavirenz and Nevirapine have been shown to promote HIV-1 RT maturation at the level of the Gag-Pol protein and to affect viral protease (PR) activation, resulting in the suppression of viral release from infected cells (30,31). Conversely, NNRTIs such as TSAO and BBNH derivatives act as destabilizers of RT subunit interaction (27).

We have demonstrated that preventing or controlling RT dimerization constitutes an alternative strategy to block HIV proliferation and has a major impact on the viral cycle (32). In protein-protein interactions the binding energy is not evenly distributed across the dimer interface but involves specific residues “hot spots” that stabilize protein complexes. We have shown that the use of small peptides targeting “hot spot” residues required for RT-dimerization constitutes a new strategy to inhibit HIV-1 RT (16,17) and have described a decapeptide “Pep-7” mimicking p66/p51 interface that prevents RT-dimerization by destabilizing RT subunit-interactions and that blocks viral replication (23,32).

The thumb domain plays an important role in the catalysis and integrity of the dimeric form of RT, thereby constituting a potential target for the design of novel antiviral compounds (7,8,22). The p66-thumb domain is involved in p/t binding and polymerase activity of RT (7,8,13) and p51-thumb domain is required for the conformational changes associated with RT dimer-maturation (22). We have designed a peptide, Pep-A, derived from a structural motif located between residues 284 and 300, corresponding to the end of helix αI, the loop connecting helices αI and αJ and a part of helix αJ. This peptide is a potent inhibitor of RT interfering with the conformational change associated with full activation of the enzyme. However, although it significantly blocks RT maturation *in vitro*, it lacks of antiviral activity (22). In the present work, we have designed and evaluated a series of peptides derived from the thumb subdomain of RT using Pep-A as a template. We have identified a 17-residue peptide $P_{AW,}$ which constitutes a potent inhibitor of RT-polymerase activity of HIV-1 RT *in vitro*. We have demonstrated that P_{AW} inhibits RT maturation and abolishes viral replication without any toxic side-effects. The characterization of the mechanism through which P_{AW} inhibits RT, combining steady-state and pre-steady state methods, together with size exclusion chromatography has revealed that P_{AW} only binds dimeric-RT and stabilizes it in an inactive/non processive dimeric conformation that prevents the proper binding of p/t. Taken together, these results demonstrate that conformational flexibility of HIV-1 RT during maturation constitutes an attractive target for AIDS chemotherapeutics

MATERIALS AND METHODS

Materials - Poly(rA)-oligo(dT) and ^{3}H-dTTP (1 μCi/μl) were purchased from Amersham Biosciences (Orsay, France). dTTP was from Roche Molecular Biochemicals, Roche Diagnostics (Meylan, France). MF-membrane (25 mm, 0.45 μm) filters for RT assay were purchased from Millipore (Molshein, France). Primer and template oligonucleotides were from MWG Biotech AG, (Ebersberg, Germany). A 19/36-mer DNA/DNA primer/template was used for steady-state fluorescence titration and stopped-flow experiments, with 5’-TCCCTGTTCGGGCGCCACT-3’ for the primer strand and 5’-TGTGGAAAATCTCATGCAGTGGCGCCCGAACAGGGA-3’ for a template-strand. The sequence of the template strand corresponds to the sequence

of the natural primer binding site (PBS) of HIV-1 (33). The primer was labelled at the 3'-end with 6-carboxyfluorescein (6-FAM) on thymine base. Primer and template oligodeoxynucleotides were separately resuspended in water and diluted to 100 µM in annealing buffer (25 mM Tris pH 7.5 and 50 mM NaCl). Oligonucleotides were mixed together and heated at 95°C for 3 min, then cooled to room temperature for 1h.

Expression and purification of HIV-1 RT proteins - His-tagged RTs were expressed and purified as previously described (23,34). Briefly, M15 bacteria (Qiagen Courtaboeuf, France) were separately transformed with all the constructs of p51 and p66 subunits. Cells were grown at 37 °C up to about 0.3 OD_{595}, then cultures were cooled to 20°C and induced overnight with 0.5 mM isopropyl-1-thio-β-D-galactopyranoside. Bacterial cultures expressing His-tagged p66 subunit were mixed with cultures expressing His-tagged p51 subunit to enable dimerization during sonication. For protein isolation and initial purification, the filtered supernatant was applied onto a Hi-Trap chelating column equilibrated with 50 mM sodium phosphate buffer, pH: 7.8, containing 150 mM NaCl supplemented with 50 mM imidazole. The heterodimeric p66/p51 RT was eluted with an imidazole gradient and finally purified by size-exclusion chromatography on a HiLoad 16/60 Superdex 75 column equilibrated with a 50 mM Tris pH: 7.0 buffer containing 1mM EDTA and 50 mM NaCl. Recombinant untagged- HIV-1 BH_{10} RT was expressed in *E.coli* and purified as previously described (35). Highly homogeneous preparations from co-expression of the p66 and p51 subunits were stored in -80°C in buffer supplemented with 50% glycerol. Protein concentrations were determined at 280 nm using a molar extinction coefficient of 260 450 $M^{-1}.cm^{-1}$.

Peptide synthesis - Pep-A derived peptides were purchased from GL Biochem, (Shanghai, China) and Genepep, SA. (Prades le Lez, France). Pep-1 and P_{AW} were synthesized using an (fluorenylmethoxy)-carbonyl (Fmoc) continuous (Pionner, Applied Biosystems, Foster city, CA) starting from Fmoc-polyamide linker (PAL)-poly(ethyleneglycol) (PEG)-polystyrene (PS) resin at a 0.05 mmol scale. Peptides were purified by semi-preparative reverse-phase high performance liquid chromatography (RP-HPLC; C18 column Interchrom UP5 WOD/25M Uptisphere 300 5 ODB, 250 mm x 21.2 mm) and identified by electrospray mass spectrometry. P_{AW} (1 mM) was coupled to FITC using maleimide-FITC (Molecular Probes. Inc.) (5 mM) through overnight incubation at 4°C in Phosphate Buffer Saline (PBS: GIBCO BRL). Fluorescently labelled peptide was further purified by RP-HPLC using a C18 reverse-phase HPLC column (Interchrom UP5 HDO/25M Modulo-cart Uptisphere, 250 mm x 10 mm) then identified by electrospray mass spectrometry.

RT-polymerase Assay – RNA-dependent-DNA RT-polymerase activity was measured in a standard reaction assay using poly(rA)-$(dT)_{15}$ as template/primer as previously described (5). Briefly, ten microliters of RT at 20 nM was incubated at 37 °C for 30 min with 20 μL of reaction buffer (50 mM Tris, pH 8.0, 80 mM KCl, 6 mM $MgCl_2$, 5 mM DTT, 0.15 μM poly(rA-dT), 15 μM dTTP, 0.3 μCi 3H-dTTP). For peptide evaluation, HIV-1 RT was incubated with increasing concentrations of peptide inhibitors for 23 hrs, and polymerase reaction was initiated by adding reaction buffer. Reactions were stopped by precipitation of nucleic acids with 5 ml of 20% trichloroacetic acid (TCA) solution for 2 h on ice, then filtered using a multiwell-sample collector (Millipore), and washed with 5% TCA solution. Filters were dried at 55°C for 30 min and radionucleotide incorporation was determined by liquid scintillation spectrometry. Data were fitted using a Dixon plot reporting the reciprocal of the velocity (1/v) as a function of inhibitor concentrations. Ki values for the different peptides were estimated from the intercept on the concentration axis (36).

Steady-State Fluorescence Experiments - Fluorescence experiments were performed in buffer containing 50 mM Tris-HCl, pH 8.0, 50 mM KCl, 10 mM $MgCl_2$ and 1 mM DTT, at 25°C, using a SPEX-PTI spectrofluorimeter in a 1 cm path-length quartz cuvette, with a band-pass of 2 nm for excitation and emission, respectively. Excitation was performed at 492 nm and emission spectra were recorded from 500 to 600 nm. According fluorescence experiments, a fixed concentration of FAM-labelled (19/36) p/t (50 nM) or of FITC-P_{AW} (200 nM) was titrated with increasing protein concentrations from 5 nM to 1 µM. Data were fitted as previously described (34,37), using a quadratic equation (GraFit, Erithacus Software).

HPLC Size Exclusion Chromatography - Chromatography was performed using one

(Phenomenex S3000) or two HPLC columns in series (Phenomenex S3000 followed by Phenomenex S2000; both 7.5 mm x 300 mm). Samples containing 3 to 10 µM of RT or p51 were applied onto one or two HLPC columns and eluted with 200 mM potassium phosphate (pH: 7.0) at a flow rate of 0.5 $ml.min^{-1}$ (5).

Rapid kinetic experiments - Binding kinetics of p/t onto HIV-1 RT were performed with a FAM – labelled p/t in buffer containing 50 mM Tris-HCl, pH 8.0, 50 mM KCl, 10 mM $MgCl_2$ and 1 mM DTT, using a stopped-flow apparatus (Hi-Tech Scientific, Salisbury, England-UK) at 25°C. A fixed concentration of FAM-labeled p/t (20 nM) was rapidly mixed with increasing concentrations of RT or RT/P_{AW} complex formed at a 1/20 molar ratio (25 to 400 nM). 6-FAM-fluorescence was excited at 492 nm and emission detected through a filter with a cut-off at 530 nm. Data acquisition and analysis were performed using KinetAsyst 3 software (Hi-Tech Scientific, Salisbury, England-UK) and traces were fitted according to a three exponential equation, as previously described (34). The rate constant for the first phase (k_{+1} and k_{-1}), corresponding to the formation of a RT/P_{AW}-p/t collision complex, was extrapolated from the slope and the intercept with the y axis of the plot of k_{obs1} vs RT concentrations. The k_2 ($k_{+2} + k_{-2}$) and k_3 ($k_{+3} + k_{-3}$) rate constants for the second and third phases corresponding to conformational changes of preformed RT/P_{AW}-p/t complex were directly obtained from the three exponential fitting.

Dissociation kinetics of HIV-1 RT were monitored by using bis-ANS as extrinsic probe Changes in bis-ANS fluorescence provide a good signal to probe variation in the exposure of the hydrophobic regions associated to RT dissociation in a time-dependent manner. 0.5µM of RT was dissociated in presence of 0.8 µM of bis-ANS, by adding 10 % acetonitrile in the absence or in the presence of 10 µM P_{AW}. Kinetics of dissociation were monitored by following fluorescence resonance energy transfer between tryptophan residues of RT and bis-ANS. Excitation of RT-Trp residues was performed at 290 nm and the increase of bis-ANS fluorescence emission at 490 nm was detected through a 420 nm cut-off filter. Data acquisition and analysis were performed using KinetAsyst 3 software (Hi-Tech Scientific, Salisbury, England-UK) and traces were fitted according to a single exponential equation.

Cell Culture, transfection and indirect immunofluorescence microscopy - HeLa cells were cultured in Dulbecco's modified Eagle's medium supplemented with 10% fetal calf serum at 37°C in a humidified atmosphere containing 5% CO_2.). Cells were grown on glass coverslips to 75% confluency, then transfected with pcDNA3-p66RT plasmid using Lipofectamine 2000 reagent according to manufacturer'instructions (Invitrogen). For colocalization experiments, cells were subsequently cultured for 32h, before incubation with FITC-P_{AW} or FITC-P_{AW}/Pep-1 (complex obtained at a molar ratio 1/10) for 1 h. Coverslips were extensively rinsed with PBS and cells were fixed in 4% paraformaldehyde for 10 min and permeabilized in 0.2% Triton. After saturation in PBS supplemented with bovine serum albumine 1% for 1h, cells were incubated overnight with monoclonal 8C4 anti-HIV-1 RT antibody (AIDS Research Reference Reagent Program, NIH) (diluted 1:100 in PBS-BSA 1%), followed by Alexa-555 anti-mouse (Molecular Probes). Immunofluorescence detection of HIV-1 RT and FITC-P_{AW} was performed by epifluorescence microscopy using a PL APO 1.4 oil PH3 objective on a LEICA DMRA 1999 microscope. 3D reconstitution of the 20 frames (interval 0.3 µm) realized from z stacking was performed using Imaris 6.0 software.

ATCC H9 cells, stably transfected with pNL4.3 V-R+ plasmid and constitutively expressing Gag-Pol HIV-1 proteins (obtained from Dr. R.Marquet-IPBS, France) were used for RT pull-down experiments. H9 cells were cultured in RPMI-1640 medium supplemented with 2mM glutamine, 10% (w/v) foetal calf serum (FCS), 1% antibiotics (streptomycin 10 000 mg/ml, penicillin, 10 000 IU/ml) and G418 (1 mg/ml). P_{AW} was incubated with 500 µl of activated CNBr-activated Sepharose 4B beads at 4°C overnight. After centrifugation, supernatants were removed and the beads were incubated with Glycine pH.8.0 for 2 hrs at 4°C with gentle stirring. The beads were then washed with 0.1 M sodium acetate buffer (pH 4.0), then 0.5 M Bicarbonate buffer, and finally in PBS, three times each. The peptide bound to the beads were then saturated for 30 min in PBS/BSA 0.1% and then incubated for 1h at 4°C with equal amounts of H9 cells lysed for 30 min on ice in Lysis buffer (Tris 20 mM, pH 7.2, NaCl 400 mM, EDTA 1mM, DTT 1mM, Protease inhibitors EDTA free) and sonicated 2 x 5 sec. at 20%. Beads were washed with Lysis buffer then twice with PBS and the bound proteins were finally separated on 15% SDS-PAGE gel and analyzed by Western Blotting using monoclonal 8C4 anti-HIV-1 RT antibody.

Antiviral assay - The anti-HIV activities of the whole series of peptides were assayed according to previously described methods (38). Phytohemagglutinin-P (PHA-P)-activated peripheral blood mononuclear cells (PBMC) were infected with the reference lymphotropic HIV-1-LAI strain (39). Virus was amplified *in vitro* on PHA-P-activated PBMC. Viral stock was titrated using PHA-P-activated PBMC, and 50% tissue culture infectious doses ($TCID_{50}$) were calculated using Kärber's formula (40). PBMC were pre-treated for 1 hr with increasing concentrations of peptide (from 100 to 0.1 nM), then infected with 100 $TCID_{50}$ of the HIV-1-LAI strain. Peptides were maintained throughout the culture, and cell supernatants were collected at day 7 post-infection and stored at −20 C. Viral replication was measured by quantifying RT activity in cell culture supernatants. In parallel, cytotoxicity of the compounds was evaluated in uninfected PHA-P-activated PBMC by colorimetric 3-(4-5 dimethylthiazol-2-yl)2,5 diphenyl tetrazolium bromite (MTT) assay on day 7 (41). Experiments were performed in triplicate and repeated with another blood donor. Data analyses were performed using SoftMax®Pro 4.6 microcomputer software: percent of inhibition of RT activity or of cell viability were plotted vs concentration and fitted with quadratic curves; 50% effective doses (ED_{50}) and cytotoxic doses (CD_{50}) were calculated.

RESULTS

Design and evaluation of Pep-A derived peptides – We have previously demonstrated that the thumb domain of p51 subunit is involved in activation of heterodimeric RT and that a 17 residue peptide, Pep-A, corresponding to an extremely well conserved structural motif located between amino acid "284-300", can affect the maturation of HIV-1 RT (22). In order to optimize and identify major residues in Pep-A required for RT inhibition, a series of new peptides have been derived from Pep-A sequence (RGTKALTEVIPLTEEAEC). First, the N-terminal arginine of Pep-A was removed to improve the solubility and facilitate the synthesis of Pep-A-derived peptides, then additional peptides were then generated by performing an alanine scan on P1. Pep-A-derived peptides were evaluated using a standard polymerase RT assay and Ki values extrapolated using Dixon plot analysis (36) are reported in Table 1.

All peptides affected the polymerase activity of RT in a dose-dependent manner, and four peptides P1 (Ki : 7.5 μM), P6 (Ki : 5.7 μM), P10 (Ki : 7.3 μM) and P11 (Ki : 7.0 μM) possess an inhibition constant lower than 10 μM (Figure 1). As a reference, we show that Pep-A inhibits RT-polymerase activity with an inhibition constant value of 35 μM. Peptide analysis reveals that removing the Arg^1 residue in Pep-A increases the potency of the peptide (P1) 5-fold. In comparison to P1, mutation of residues Gly^1, Ala^4, Glu^7, and Leu^{11} into alanine significantly affects the potency of the peptide suggesting that the side chains of these residues are required for the interaction with RT. The nature of the side chain of Glu^7 seems to be a major requirement for the interaction with RT as its substitution by Alanine (P8), reduces the efficiency of the peptide 8 fold. In contrast, Lys^3, Thr^6, Val^8 and Glu^{14} residues have a minor impact as their mutation into alanine only reduces their potency by a factor of 2. Interestingly, the hydrophobic character of Ala^4 and Val^8 side chains plays a role in the binding of the peptide to RT and reducing their length affects the potency of the corresponding peptides to inhibit RT 2.7- and 2-fold, respectively. Taking into account that Trp residues are generally involved in stabilisation of protein/protein interfaces, the two residues Ala^4 and Val^8 were mutated into Trp, to favour the binding of the peptide to RT. As shown in Figure 1, the corresponding peptide P_{AW} significantly inhibits RT polymerase activity with an inhibition constant (Ki) of 0.7 μM, revealing that mutation of these two residues into Trp improves peptide efficiency 50-fold over Pep-A and 10-fold in comparison to the best lead peptide from the Ala-scan (P6) (Figure 1, Table 1).

Antiviral potency of Pep-A derived peptides - Antiviral activity of the five peptide leads (P1,P6, P10, P11, P_{AW}) was evaluated on PHA-P-activated PBMC infected with HIV-1 LAI Results were reported as 50% efficient concentration (EC_{50}) and selectivity index corresponding to the ratio between EC_{50} and the cytotoxic concentration (CC_{50}) inducing 50% death of uninfected PBMCs and relative to Pep-A and P8 (Table 2). In order to avoid any limitation due to the poor ability of peptides to cross cellular membranes, they were associated to the peptide-based nanoparticle delivery system Pep-1, at a 1/10 molar ratio. Pep-1 has been successfully used for the delivery of peptides and proteins into numerous cell lines as well as i*n vivo* (42,43). The inability of free peptides to block viral replication is directly

associated to their poor cellular uptake as reported in Figure 2A for fluorescently-labelled peptide (FITC-P_{AW}). In contrast, when complexed at a molar 1/10 ratio with Pep-1 delivery system, FITC-P_{AW} rapidly (in less than 1h) enters cells (Figure 2B). FITC-P_{AW} localization and RT/P_{AW} interaction were characterized using 3D reconstitution of frames from z stacks. 3D image analysis reveals that P_{AW} does not enter the nucleus and partially localizes with RT at the periphery of the nucleus (Figures 2E & 2F).

When associated with Pep-1, peptides P1, P6, P10 and P11 block viral proliferation with IC_{50} values in the low µM range, which correlates with their ability to inhibit HIV-1 RT *in vitro* (Table 2). In contrast, in agreement with previous findings no antiviral activity was observed with Pep-A when associated to Pep-1 (22). When complexed with Pep-1, P_{AW} exhibits a marked antiviral activity with an EC_{50} of 1.8 nM and a therapeutic/selectivity index of about 550. The 44- and 161-fold greater potency of P_{AW} over peptides harbouring mutations at Glu^7 (P8) or lacking Trp residues (P1) confirms the requirement of these residues for targeting RT both *in vitro* and *in cellulo*. P_{AW} constitutes a powerful inhibitor of polymerase activity and possesses a very potent antiviral activity without any toxic effect. We therefore, further investigated its mechanism of action on RT.

P_{AW} peptide interacts with HIV-1 RT in a cellular context - To confirm that P_{AW} targets HIV-1 RT in a cellular context, we further investigated its ability to form stable complexes with HIV-1 RT expressed in cells was investigated by pull-down experiments. The peptides P_{AW} and P8 covalently associated with CNBr sepharose beads, was incubated in the presence of cell lysates of H9 cells expressing Gag-Pol gene products of HIV-1. Analysis of the presence of RT by Western blotting reveals than only P_{AW} was able to form stable complex with RT in a cellular context and to retain RT on beads (Figure 2G). In contrast, no RT was associated to free or P8-beads.

Binding of P_{AW} peptide to the dimeric form of HIV-1 RT. To further understand the mechanism through which P_{AW} inhibits RT, we investigated its potency to interact with the dimeric form of HIV-1 RT in the absence or presence of DNA/DNA p/t. The binding of P_{AW} to RT was monitored using a fluorescently labelled peptide (FITC-P_{AW}). We first evaluated the impact of P_{AW} labelling on the C-terminal cysteine with an FITC-probe on its ability to inhibit RT polymerase activity. As reported in Table 1, FITC-P_{AW} blocks RT polymerase activity with a Ki of 2.7 ± 0.7 µM, 3.8-fold greater than for P_{AW}, suggesting that labelling has only a minor effect on P_{AW} inhibitory property. As reported in Figure 3A, upon binding to the dimeric form of RT, the fluorescence of FITC-P_{AW} was quenched by 39 % and analysis of the titration curves revealed that P_{AW} tightly binds heterodimeric RT with a dissociation constant (Kd) of 33 ± 10 nM. When RT is first incubated with DNA/DNA p/t (18/36 mer), the quenching of FITC-P_{AW} fluorescence associated with its binding was of 57% and the affinity of FITC-P_{AW} for RT increased 5-fold (Kd : 7.1 ± 2.8 nM), suggesting that the presence of p/t on RT facilitates the binding of P_{AW}. The association of unlabelled P_{AW} to RT was also evaluated by monitoring changes in fluorescently labelled p/t bound to RT (Figure 3B). Binding of P_{AW} results in a 39 % quenching of fluorescence and a Kd value of 40 ± 18 nM was estimated from the titration binding curve. The 5.6-fold lower Kd of labelled FITC-P_{AW} over unlabelled peptide, suggests that the dye contacts RT and stabilizes the peptide within its binding site.

As both Trp^{24} and Phe^{61} located on the fingers domain of p66 subunit have been reported to be involved in the control of p/t binding and in the dynamics of the thumb-fingers subdomain interactions (34,44,45), we then evaluated the binding of P_{AW} on RT harbouring single Phe^{61Gly} and double Phe^{61Gly} and Trp^{24Gly} mutations on the p66 subunit. In comparison to wild type RT, the affinity of P_{AW} was reduced 6-fold (Kd : 207 ± 62 nM) for $p66^{F61G}/p51^{wt}$ and 4.5-fold (Kd : 149 ± 38 nM) for $p66^{DM}/p51^{wt}$ (Figure 3A).

Effect of P_{AW} peptide on primer/template binding to HIV-1 RT - The impact of P_{AW} peptide on the ability of HIV-1 RT to bind p/t was then investigated at both steady-state and pre-steady state levels using a 19/36 mer p/t labelled at the 3'-end of the primer with FAM-derivative as previously described (34,37). As reported in Figure 4A, the presence of a saturating concentration of P_{AW} (10 µM) decreases the affinity of fluorescently labelled-p/t for RT 4.5-fold with a Kd value of 99 ± 40 nM in comparison to 22 ± 5 nM obtained in the absence of P_{AW}. The binding of unlabeled p/t induces a 42 % change in the fluorescence of P_{AW}-FITC pre-bound to RT and leads to a similar Kd value of 66.5 ± 19 nM (Figure 4A). These results suggest that p/t interacts close to P_{AW} binding site on RT, inducing a change in the orientation of

FITC linked to P_{AW}, but does not share the same binding site.

RT-p/t pre-steady-state binding kinetics follow a three-step mechanism in the presence or in the absence of P_{AW}, including a rapid diffusion controlled second order step leading to the formation of the RT-p/t collision complex, followed by two slow, concentration-independent, conformational changes (34). The plot of the pseudo-first order rate constant for the initial association of the p/t with RT against RT-concentration is linear. In the absence of P_{AW}, k_{+1} and k_{-1} rate constant values of $4.23 \cdot 10^8$ $M^{-1} \cdot s^{-1}$ and 29.9 s^{-1} were calculated from the slope and the intercept with the y axis of the graph (Figure 4B & 4C). Analysis of the second and third slow phases yielded rate constants of $k_2 = 5.8$ s^{-1} and $k_3 = 0.76$ s^{-1} for RT. The presence of P_{AW} does not alter the overall Kd1 for the initial formation of the RT-p/t complex as both the "on" ($k_{+1} = 1.05 \cdot 10^8$ $M^{-1} \cdot s^{-1}$) and the "off" ($k_{-1} = 7.9$ s^{-1}) rates of the first step are decreased by about 4-fold. In contrast, the presence of P_{AW} on RT significantly reduced the rate constants of the slow conformational steps ($k_2 = 1.99$ s^{-1} and $k_3 = 0.22$ s^{-1}), affecting the proper binding of the p/t (Figure 4B & 4C).

Effect of P_{AW} on the stability and dimerization of HIV-1 RT - The impact of P_{AW} on the stability and formation of heterodimeric-RT was investigated in detail by size-exclusion chromatography as previously described (17). As reported in Figure 5A, heterodimeric-RT incubated or not in the presence of an excess of P_{AW} (100µM) for 1h30 at room temperature, is fully dimeric and eluted as a single peak at 16.7 min. The interaction of P_{AW} with RT was monitored by size-exclusion chromatography using HIV-1 RT pre-incubated with FITC-P_{AW}. Chromatography analysis reveals that FITC-P_{AW} co-elutes with heterodimeric RT in a single peak at 16.7 min (Figure 5A), demonstrating that P_{AW} binds heterodimeric RT and does not induce RT dissociation. We then evaluated the ability of P_{AW} to interact with p66 or p51 monomeric forms. Experiments performed with a partially dissociated RT/P_{AW} (50%) complex by 10% acetonitrile, show that P_{AW} remains associated only with the dimeric fraction of RT, and does not bind monomeric p66 or p51 subunits, which are eluted at 17.5 min and 18.2 min, respectively(Figure 5B).

We then investigated the ability of P_{AW} to prevent HIV-1 RT-dimerization. Dissociation of RT was achieved at room temperature with 17% acetonitrile, and then association of the subunits was induced by a 10-fold dilution of the sample in an acetonitrile-free buffer in the absence or presence of 100 µM of P_{AW}. At this concentration (1.7%) of acetonitrile no dissociation of RT could be detected. As shown in Figure 6A, heterodimeric RT was fully re-associated 5 hrs after dilution in an acetonitrile-free buffer, both in the absence or in the presence of P_{AW} (100 µM), indicating that P_{AW} does not block RT dimerization (Figure 6A). The impact of P_{AW} was further investigated on the kinetics of RT-dimerization. The level of dimeric RT was evaluated 30 min and 2 hrs after dilution in free acetonitrile buffer by size-exclusion chromatography (Figure 6B & 6C). In the presence of P_{AW} 21 % and 59 % of dimeric RT was quantified after 30 min and 2 hrs respectively (Figure 6B). In comparison only 16 % (30 min) and 29 % (2hrs) of dimeric RT were detected in the absence of peptide (Figure 6C), suggesting that the presence of P_{AW} favours the kinetics of RT dimerization.

P_{AW} peptide favours dimerization of the small p51 subunit - P51 subunits are mainly monomeric and dissociation constants for p51/p51 homodimer have been reported to be either in the µM (25) or mM (5) range depending on the technology used to quantify the interactions. We have investigated the ability of P_{AW} to favour p51/p51 dimerization by size exclusion chromatography, using two HPLC columns in series. Experiments were performed at a p51 concentration of 3.5 µM at which it is entirely monomeric and elutes as a single peak at 32.7 min (Figure 7). Monomeric p51 (3.5µM) was incubated in the presence of FITC-labelled P_{AW} (20 µM) for 1 h at room temperature then analysed by size exclusion chromatography. As reported in Figure 7, in the presence of fluorescently-labelled P_{AW} 4.6 % of p51 are dimeric and associated to P_{AW}, suggesting that P_{AW} promotes p51/p51 homodimer and only p51/p51 homodimer.

P_{AW} peptide prevents HIV-1 RT dissociation - Finally, the impact of P_{AW} on HIV-1 RT stability and dissociation were investigated at the steady state level by size exclusion chromatography and at the pre-steady state level by stopped-flow rapid kinetics. HIV-1 RT was preincubated in the presence of 100 µM P_{AW}, for 2hr, prior dissociation with 17% or 10 % of acetonitrile, and the level of dimeric form was then assessed by size exclusion chromatography and the rate of dissociation by pre-steady-state kinetics. As reported in Fig 8A, the presence of P_{AW} protects

RT from the acetonitrile dissociation as 17% remains dimeric whereas "free" RT is completely dissociated with 17% acetonitrile.

The protection by P_{AW} of acetonitrile-associated RT-dissociation was further investigated by monitoring pre-steady-state dissociation kinetics of HIV-1 RT, using bis-ANS as an extrinsic probe (46). Binding of bis-ANS to dissociated RT resulted in a large increase in the fluorescence of the probe due to non covalent interactions of bis-ANS to exposed hydrophobic surfaces on RT subunits, therefore providing a good signal for following RT dissociation in a time-dependent manner. Experiments were performed by adding bis-ANS to HIV-1 RT prior dissociation of the enzyme by 10% acetonitrile and monitoring FRET between exposed Trp of RT and Bis-ANS. As reported in Figure 8B, the kinetics of increased ANS-fluorescence upon dissociation of RT in the absence of P_{AW} follow a single-exponential reaction, with a dissociation rate constant k_{dis} of 5.30 ± 0.01 s^{-1}, which is reduced 3.8-fold (k_{dis} =1.42 ± 0.007 s^{-1}), when RT is incubated with P_{AW}

Optimization of P_{AW} and selection of a minimal inhibitory peptide-motif - Taken together our results demonstrate that P_{AW} constitutes a potent conformational inhibitor of RT and exhibits a potent antiviral activity. To define the minimal peptidic sequence for RT inhibition, new peptides derived from P_{AW} were designed and evaluated (Table 3). As the interaction between P_{AW} and RT seems to involve both the N-terminal part and Trp-residues of the peptide, the peptidic-sequence was shortened at the N and/or C-terminal extremities and the positional effect of the Trp was evaluated. All peptides were tested in standard RT assays (Table 3) and were evaluated on PBMC infected by HIV-1 LAI (Table 2). Reducing P_{AW} sequence by 2 residues at the N-terminus reduced efficiency 2.5 fold (P26 : Ki= 1.8 ± 0.7 µM). In contrast, the 5 last residues at the C-terminus of P_{AW} can be removed without affecting its potency to inhibit RT polymerase activity or to block viral replication (P24 : Ki= 0.7 ± 0.05 µM and EC_{50} = 2.3 nM). That P18 does not inhibit RT polymerase activity, confirms that the Trp residues form the major interface with RT. Moving Trp^8 to position 9 (P16) and both Trp^4 and Trp^8 to position 5 and 9 (P17) reduced the efficiency of the corresponding peptides 20-fold (Ki : 14 ± 4 µM) and 50-fold (Ki : 35 ± 11 µM), respectively. Interestingly, removing the last two residues of P_{AW} increases its efficiency 14-fold (P27 : Ki= 50 ± 0.01 nM) and is also associated with an increase in its antiviral activity with an IC_{50} lower than 0.32 nM and a therapeutic/selectivity index greater than 3100.

DISCUSSION

Targeting the conformational flexibility of heterodimeric RT has provided new concepts for the design of drugs active on viruses resistant to currently used RT-inhibitors (5,17,26,28,47). RT activation involves a two-step dimerization process initiated by a rapid monomer/monomer association generating an inactive intermediate heterodimer, followed by a slow isomerization yielding the biologically active enzyme (5,20). Considering that HIV-1 RT is extremely stable (25,46,48), selection of compounds that are able to dissociate the complex remains challenging. In contrast, as maturation of RT requires less energy than dimerization, targeting conformational changes involved is a very attractive approach for the design of novel antiviral compounds. Maturation of the inactive intermediate heterodimer corresponds to conformational changes involving interactions between the thumb of p51 and the RNAse H of p66 and between the fingers of p51 and the palm of p66 (20). We previously demonstrated that the thumb domain of p51 plays a major role in RT-maturation and that a synthetic peptide (Pep-A) derived from this domain selectively inhibited activation of HIV-1 RT (22). In the present work, we report the design of a new generation of peptide inhibitors derived from the thumb domain and have identified a lead peptide P_{AW} that efficiently blocks both maturation of RT and viral replication.

P_{AW} peptide preferentially binds dimeric RT in the "open" conformation - From size exclusion chromatography, we clearly demonstrated that P_{AW} only binds dimeric forms of RT (p66/p51 and p51/p51). Moreover, as already reported for Pep-A (22), P_{AW} does not induce heterodimer dissociation nor prevent the monomer/monomer association, and instead significantly increases stability of the heterodimer and favours dimerization. According to the two step process mechanism, we propose that P_{AW} blocks RT maturation by stabilizing the inactive intermediate of RT in a non processive conformation.

Determination of crystal structures of the HIV-1 RT associated or not with a p/t has revealed that the binding of p/t to RT triggers major conformational changes in the overall structure of

the enzyme, including the increase in the compactness together with conversion of RT from a "closed" to an "open" conformation (7-9). The structure RT adopts two conformational states: a "closed" conformation stabilized by interactions between fingers and thumb domains of p66 and an "open" conformation associated with a change in the orientation of the thumb domain and a shift of the fingers domain which are induced by p/t binding (8,9). We demonstrate that P_{AW} tightly binds RT preferentially in the "open" conformation, as its affinity is increased 5-fold in the presence of p/t. The dynamics of the thumb and fingers domains of p66 and the conformational changes of RT associated with p/t binding exposes the binding site of P_{AW}, was strengthened by the fact that mutation of Phe^{61} into glycine on the fingers domain of p66 subunit altered binding of P_{AW} to RT (6-fold). Phe^{61} is located in the fingers domain and together with Trp^{24} and Arg^{78} is involved in the stabilization of the "closed" conformation of RT, by contacting the loop between helices αI and αJ of the thumb domain. Given that mutation of Phe^{61} favours the "open" conformation of RT (34), but dramatically reduces the affinity of P_{AW} for RT, suggests that this residue is directly involved in the binding of P_{AW}. And that P_{AW} binding site is located close to this residue on either the thumb or fingers domain of p66.

P_{AW} peptide blocks RT in an inactive conformation altering proper binding of primer/template - The initial monomer/monomer interaction yields an intermediate dimer lacking of polymerase and RNAse H activities, then corrected organisation of the catalytic and the p/t binding sites occurs during a slow maturation step (20). We propose that P_{AW} interacts directly with the intermediate inactive form which stabilizes in a non-processive conformation. From a mechanistic point of view, P_{AW} acts as non-competitive inhibitor affecting conformational changes required for proper folding of the p/t binding site. P_{AW} does not displace RT:p/t complex but reduces both "off" and "on" rates of the collisional binding of p/t to RT, it does not affected the overall dissociation constants of the collisonal step, with K1 values of 70.4 nM and 70.6 nM obtained in the presence or the absence of P_{AW}, respectively. In contrast, P_{AW} dramatically affects the proper binding and conformational changes that place correctly the p/t for catalysis. The corresponding rate constants are reduced by 3-fold (k_2) and 3.4 fold (k_3), respectively. Taken together that P_{AW} binds heterodimeric and homodimeric RTs (p66/p51 and p51/p51), preferentially in the "open" conformation, and that it specifically inhibits polymerase activity and not RNAse H, demonstrates that P_{AW} interacts with the inactive intermediate form of RT and prevents conformational changes required for the proper folding of the p/t binding site.

Similarly, NNRTIs are non competitive inhibitors that block RT in a non processive conformation (24-28). NNRTIs bind near the RT-polymerase catalytic site and affect the dynamics of thumb/finger domain interaction on p66 subunit and maintain RT in an "open" conformation (6,8,10). Although the molecular mechanism by which NNRTIs inhibit RT is not entirely clear, evidence reports that binding of NNRTIs restricts the mobility of the thumb domain, slowing or preventing p/t translocation and thereby inhibiting elongation of nascent DNA. NNRTIs such as efavirenz favour RT dimerization *in vitro* and in cultured cells (24), but in contrast to P_{AW}, they improve the binding of p/t (35,50), which excludes that P_{AW} and NNRTI binding sites overlap and favours a P_{AW} binding site close to the interface between the thumb and fingers domain of p66.

P_{AW} is potent antiviral compound - When associated with Pep-1-based nanoparticles, P_{AW} is a potent non toxic inhibitor of viral replication (EC_{50}: 1.8 nM). This peptide constitutes a major improvement in comparison to Pep-A which is 50-fold less potent *in vitro* on RT activity and does not exhibit any antiviral activity in the same delivery conditions. We demonstrate that when delivered into cells using Pep-1, P_{AW} interacts with RT in both cells expressing only p66 and in the context of the full Pol-polyprotein. Taking together this result with the fact that P_{AW} EC_{50} values on HIV-LAI are similar to its dissociation constant for RT, confirms that P_{AW} inhibition occurs via conformational changes on RT and not through direct inhibition of polymerase activity. The analysis of P_{AW} sequence has revealed that essential residues involved in RT binding and antiviral activity are located in the N-terminus of the peptide. In particular, Glu^7, Leu^{11}, Trp^4 and Trp^8 are required for binding of P_{AW} to RT. The hydrophobic character of the side chain of Trp-residues at position 4 and 8 plays a major role in stabilizing P_{AW}/RT complex. We show that P_{AW} can be reduced to 12 residues (P24) without affecting either its *in vitro* or *in cellulo* potency. Interestingly, removing the last two residues of P_{AW} (P27) increases *in vitro* and antiviral

efficiency 12-fold and 10-fold, respectively. These results suggest that although the Trp residues are key residues for the potency of the peptide, residues 12 to 14 in the sequence of P_{AW} are also required to stabilize P_{AW} in its binding site.

Conclusions - In the present work, we have demonstrated that the dynamics of the finger/thumb domains of p66 play an essential role in the stabilisation and maturation of heterodimeric HIV-1 RT. As such, we have established a proof of concept that targeting conformational changes required for RT flexibility can lead to highly potent antiviral molecules. We have identified a new RT inhibitor, P_{AW} which alters finger/thumb dynamics and maintains RT in a non-processive conformation, by altering the proper binding of p/t to RT. Development of this type of inhibitor together with a better knowledge of its mechanism at the viral level will provide new perspectives for designing specific inhibitors of the "niche" of highly resistant strains.

REFERENCES

1. Simon, V., Ho, D. D., and Abdool Karim, Q. (2006) *Lancet* 368, 489-504
2. di Marzo Veronese, F., Copeland, T. D., DeVico, A. L., Rahman, R., Oroszlan, S., Gallo, R. C., and Sarngadharan, M. G. (1986) *Science* 231, 1289-1291
3. Lightfoote, M. M., Coligan, J. E., Folks, T. M., Fauci, A. S., Martin, M. A., and Venkatesan, S. (1986) *.J. Virol* 60, 771-775
4. De Clercq, E. (2007) *Nat Rev Drug Discov* 6, 1001-1018
5. Restle, T., Muller, B., and Goody, R. S. (1990) *J Biol Chem* 265, 8986-8988
6. Kohlstaedt, L. A., Wang, J., Friedman, J. M., Rice, P. A., and Steitz, T. A. (1992) *Science* 256, 1783-1790
7. Jacobo-Molina, A., Ding, J., Nanni, R. G., Clark, A. D., Jr., Lu, X., Tantillo, C., Williams, R. L., Kamer, G., Ferris, A. L., Clark, P., and et al. (1993) *Proc Natl Acad Sci U S A* 90, 6320-6324
8. Huang, H., Chopra, R., Verdine, G. L., and Harrison, S. C. (1998) *Science* 282, 1669-1675
9. Rodgers, D. W., Gamblin, S. J., Harris, B. A., Ray, S., Culp, J. S., Hellmig, B., Woolf, D. J., Debouck, C., and Harrison, S. C. (1995) *Proc Natl Acad Sci U S A* 92, 1222-1226
10. Hsiou, Y., Ding, J., Das, K., Clark, A. D., Jr., Hughes, S. H., and Arnold, E. (1996) *Structure* 4, 853-860
11. Wang, J., Smerdon, S. J., Jager, J., Kohlstaedt, L. A., Rice, P. A., Friedman, J. M., and Steitz, T. A. (1994) *Proc Natl Acad Sci U S A* 91, 7242-7246
12. Ghosh, M., Jacques, P. S., Rodgers, D. W., Ottman, M., Darlix, J. L., and Le Grice, S. F. (1996) *Biochemistry* 35, 8553-8562
13. Wohrl, B. M., Krebs, R., Thrall, S. H., Le Grice, S. F., Scheidig, A. J., and Goody, R. S. (1997) *J Biol Chem* 272, 17581-17587
14. Patel, P. H., Jacobo-Molina, A., Ding, J., Tantillo, C., Clark, A. D., Jr., Raag, R., Nanni, R. G., Hughes, S. H., and Arnold, E. (1995) *Biochemistry* 34, 5351-5363
15. Huang, S. C., Smith, J. R., and Moen, L. K. (1992) *Biochem. Biophys Res. Commun.* 184(2), 986-992
16. Divita, G., Restle, T., Goody, R. S., Chermann, J. C., and Baillon, J. G. (1994) *J Biol Chem* 269, 13080-13083
17. Divita, G., Baillon, J. G., Rittinger, K., Chermann, J. C., and Goody, R. S. (1995) *J Biol Chem* 270, 28642-28646
18. Camarasa, M. J., Velazquez, S., San-Felix, A., Perez-Perez, M. J., and Gago, F. (2006) *Antiviral Res* 71(2-3), 260-267
19. Sticht, J., Humbert, M., Findlow, S., Bodem, J., Muller, B., Dietrich, U., Werner, J., and Krausslich, H. G. (2005) *Nat Struct Mol Biol* 12, 671-677
20. Divita, G., Rittinger, K., Geourjon, C., Deleage, G., and Goody, R. S. (1995) *J Mol Biol* 245, 508-521
21. Cabodevilla, J. F., Odriozola, L., Santiago, E., and Martinez-Irujo, J. J. (2001) *Eur. J. Biochem* 268, 1163-1172
22. Morris, M. C., Berducou, C., Mery, J., Heitz, F., and Divita, G. (1999) *Biochemistry* 38, 15097-15103

23. Depollier, J., Hourdou, M. L., Aldrian-Herrada, G., Rothwell, P., Restle, T., and Divita, G. (2005) *Biochemistry* 44, 1909-1918
24. Tachedjian, G., Orlova, M., Sarafianos, S. G., Arnold, E., and Goff, S. P. (2001) *Proc Natl Acad Sci U S A* 98, 7188-7193
25. Venezia, C. F., Howard, K. J., Ignatov, M. E., Holladay, L. A., and Barkley, M. D. (2006) *Biochemistry* 45, 2779-2789
26. Sluis-Cremer, N., and Tachedjian, G. (2002) *Eur. J. Biochem.* 269, 5103-5111
27. Sluis-Cremer, N., Arion, D., and Parniak, M. A. (2002) *Mol.Pharmacol.* 62, 398-405
28. Tachedjian, G., and Goff, S. P. (2003) *Curr Opin Investig Drugs* 4(8), 966-973
29. Telesnitsky, A. G., S.P. (1997) Reverse transcriptase and the generation of retroviral DNA. . In: Coffin, J. M., Hughes, S.H., Vermus, H.E. eds (ed). *Retroviruses*, Cold Spring Harbor Laboratory Press, Plainview, NY
30. Tachedjian, G., Moore, K. L., Goff, S. P., and Sluis-Cremer, N. (2005) *FEBS Lett.* 579, 379-384
31. Figueiredo, A., Moore, K. L., Mak, J., Sluis-Cremer, N., de Bethune, M. P., and Tachedjian, G. (2006) *PLoS pathogens* 2, e119
32. Morris, M. C., Robert-Hebmann, V., Chaloin, L., Mery, J., Heitz, F., Devaux, C., Goody, R. S., and Divita, G. (1999) *J Biol Chem* 274, 24941-24946
33. Wain-Hobson, S. Sonigo, P., Danos, O., Cole, S. and Alizon, M. (1985) *Cell* 40, 9-17
34. Agopian, A., Depollier, J., Lionne, C., and Divita, G. (2007) *J Mol Biol*. 373, 127-140.
35. Muller, B., Restle, T., Weiss, S., Gautel, M., Sczakiel, G., and Goody, R. S. (1989) *J. Biol. Chem.* 264, 13975-13978
36. Dixon, M. (1952) *Biochem. J.* 55, 170-171
37 Rittinger, K., Divita, G., and Goody, R. S. (1995) *Proc Natl Acad Sci U S A* 92, 8046-8049
38. Roisin, A., Robin, J. P., Dereuddre-Bosquet, N., Vitte, A. L., Dormont, D., Clayette, P., and Jalinot, P. (2004) *J. Biol. Chem.* 279, 9208-9214
39. Barre-Sinoussi, F., Chermann, J. C., Rey, F., Nugeyre, M. T., Chamaret, S., Gruest, J., Dauguet, C., Axler-Blin, C., Vezinet-Brun, F., Rouzioux, C., Rozenbaum, W., and Montagnier, L. (1983) *Science* 220(4599), 868-871
40. Kärber. (1931) *Naunyn-Schmiedebergs Archiv für experimentelle Pathologie und Pharmakologie* 162, 480-483
41. Mossmann T (1983) *J. Immunol. Methods* 65, 55-63
42. Gros, E., Deshayes, S., Morris, M. C., Aldrian-Herrada, G., Depollier, J., Heitz, F., and Divita, G. (2006) *Biochimic et biophysica acta* 1758(3), 384-393
43. Morris, M. C., Depollier, J., Mery, J., Heitz, F., and Divita, G. (2001) *Nat.Biotech.* 19, 1173-1176
44. Fisher, T. S., Darden, T., and Prasad, V. R. (2003) *J Mol Biol* 325, 443-459
45. Fisher, T. S., and Prasad, V. R. (2002) *J Biol Chem* 277, 22345-22352
46. Divita, G., Rittinger, K., Restle, T., Immendorfer, U., and Goody, R. S. (1995) *Biochemistry* 34, 16337-16346
47. Mulky, A., Sarafianos, S. G., Arnold, E., Wu, X., and Kappes, J. C. (2004) *J Virol* 78, 7089-7096
48. Becerra, S. P., Kumar, A., Lewis, M. S., Widen, S. G., Abbotts, J., Karawya, E. M., Hughes, S. H., Shiloach, J., Wilson, S. H., and Lewis, M. S. (1991) *Biochemistry* 30(50), 11707-11719
49. Wohrl, B. M., Krebs, R., Goody, R. S., and Restle, T. (1999) *J Mol Biol* 292, 333-344
50. Divita, G., Müller, B., Immendörfer, U., Gautel, M., Rittinger, K., Restle, T., and Goody, R. S. (1993) *Biochemistry* 32, 7966-7971,

FOOTNOTES

This work was supported in part by the Centre National de la Recherche Scientifique (CNRS) and by grant from the Agence Nationale de Recherche sur le SIDA (ANRS) and SIDACTION. AA and EG were supported by fellowships of SIDACTION and of the European Community, respectively. This work is part of the program "Targeting Replication and Integration of HIV HIV" (TRIoH) supported by the EC (LSHB-CT-2003-503480). We would like to thank M. C. Morris for the pcDNA3-P66RT

clone and critical reading of the manuscript and R. Goody for HIV-RT clones. We also thank J. Cau and S. De Rossi from the Montpellier RIO Imaging facility (www.mri.cnrs.fr). Monoclonal 8C4 anti-HIV-1 RT antibobies were obtained though the AIDS Research Reference Reagent Program, Division of AIDS, NIAID, NIH.

FIGURE LEGENDS

Figure 1: Inhibition of the HIV-1 RT polymerase activity by Pep-A derived peptides. HIV-1 RT (40 nM) was incubated with increasing concentrations of Pep-A-derived peptides, P1 (●), P6 (★), P10 (■), P11 (▼) and P_{AW} (▲), then polymerase reaction was initiated by addition of a mix containing poly(rA).$(dT)_{15}$ and dTTP substrates. Inhibition constants were extrapolated from Dixon plots (36).

Figure 2: HIV-1 RT interacts with P_{AW} in cultured cells. (A-F) cellular localization of P_{AW} and its interaction with HIV-1 RT *in cellulo* was monitored using HeLa cells expressing RT transfected with FITC-P_{AW}/Pep-1 complex formed at a 1/10 molar ratio. HIV-1 RT (Alexa 555 secondary antibody) and FITC-P_{AW} were respectively visualized through a Cy3 and a GFP filter. HeLa cells transfected with free FITC-P_{AW} (A) or complexed with Pep-1 (B). Cultured Hela cells transfected (D) with pcDNA3-p66RT. HeLa cells co-transfected with both pcDNA-p66RT and FITC-P_{AW}/Pep-1 at a 1/10 molar ratio. The RT/P_{AW} co-localisation was analyzed by the 3-D image reconstitution with Imaris 6.0 software of 20 frames from z stacks (E,F). RT, P_{AW} and nuclear staining with Hoechst are reported in red, green and blue, respectively. Global view (D), 3D image analysis of a selected cell (red arrow) reveals that P_{AW} and RT localize in the cytoplasm at the periphery of the nucleus. (F) Zoom of the box reported in panel E. (G) Interaction between P_{AW} and HIV-1 RT detected in a CNBr-pull-down assay. Experiments were performed as described in Materials and Methods. 30 µg (total protein) per lane were separated on 15% SDS-PAGE and subjected to Western blotting using rabbit anti-RT antibody. Lanes correspond to control free beads, P8-, P_{AW}-beads and total proteins loaded on the gel, respectively.

Figure 3: Binding titration of FITC-P_{AW} to RT and RT-p/t. (A) Titration of FITC-P_{AW} binding to RT (○), RT:p/t (●), $p51^{wt}/p66^{F61G}$ (△) or $p51^{wt}/p66^{DM}$ (□). A fixed 200 nM concentration of FITC-P_{AW} was titrated with increasing concentrations of HIV-1 RTs or RT:p/t. The binding of P_{AW} to RT was monitored by following the quenching of extrinsic P_{AW} fluorescence at 512 nm, upon excitation at 492 nm. (B) Titration of P_{AW} binding to RT:FAM-p/t. A fixed 20 nM concentration of RT:p/t was titrated with increasing concentrations of P_{AW}. The binding of P_{AW} to RT was monitored by following the quenching of extrinsic fluorescence of FAM-labelled p/t at 512 nm, upon excitation at 492 nm. Kd values were calculated using a quadratic equation and correspond to the mean of at least three separate experiments.

Figure 4: Impact P_{AW} peptide on the binding of primer/template to HIV-1 RT. (A) Titration of fluorescently labelled p/t binding to RT (○) or RT/P_{AW} (●) and of FITC-P_{AW}/RT binding to p/t (▲). A fixed 50 nM concentration of fluorescently-labelled p/t was titrated with increasing concentrations of RT or RT/P_{AW}. The binding of p/t to RT was monitored by following the quenching of p/t extrinsic fluorescence at 512 nm, upon excitation at 492 nm. A fixed 100 nM concentration of FITC-P_{AW}/RT complex was titrated by increasing concentrations of p/t (18/36). The binding of FITC-P_{AW}/RT to p/t was monitored by following the quenching of P_{AW} extrinsic fluorescence at 512 nm, upon excitation at 492 nm. Kd values were calculated using a quadratic equation as previously described (20) and correspond to the mean of at least three separate experiments. Kinetics of binding of fluorescently labelled p/t to RT (B) and RT/P_{AW} (C). Typical stopped-flow time courses are reported, where a fixed 20 nM concentration of FAM-labelled p/t was rapidly mixed with 100 nM of RT (B) or RT/P_{AW} (C). Data collection acquisition and analysis were performed using KintAsyst 3 software and kinetics were fitted using a three exponential equation. (D) Secondary plot of the dependence of the fitted pseudo-first order rate constants for the first phase on RT (○) or RT/P_{AW} (●) concentration.

Figure 5: Binding of P_{AW} to heterodimeric RT as monitored by size-exclusion chromatography.

(A) Heterodimeric RT (2.3 µM) was incubated in the presence of P_{AW} (10 µM) for 1h30 at room temperature, then applied onto a gel filtration column and eluted with 200 mM potassium phosphate buffer, pH 7.0. (B) Heterodimeric RT (10 µM) was incubated in the presence of FITC-P_{AW} (150 µM) for 2h at room temperature then partially dissociated by 10% acetonitrile for 30 min and analyzed by gel filtration. Proteins were monitored at 280 nm (blue line) and fluorescein-labelled peptide at 492 nm (orange line).

Figure 6: Effect of P_{AW} peptide on HIV-1 RT-dimerization. (A) Impact of P_{AW} on RT-dimerization. 10 µM of RT was dissociated in the presence of 17% acetonitrile yielding 2 peaks corresponding to p66 and p51 subunits (in black), then p51 and p66 subunits were diluted in an acetonitrile free buffer and incubated overnight at room temperature in the absence (in blue) or presence of 100 µM P_{AW} (in red). Kinetics of subunit dimerization 30 min (B) and 2 hrs (C) after dilution in an acetonitrile free buffer. 10 µM of fully dissociated RT were incubated in the presence (in red) or absence of 100 µM P_{AW} (in blue), then dimerization was induced by dilution in an acetonitrile free buffer and the level of dimer/monomers was monitored at 30 min and 2 hrs by size exclusion chromatography.

Figure 7 : P_{AW} peptide favours dimerization of the small p51 subunit. HIV-1 p51 (3.5 µM) free (in blue) or incubated with FITC-P_{AW} (20 µM) (in red) were applied onto a size exclusion chromatography using two HPLC columns in series. Proteins were monitored at 280 nm and fluorescein-labelled P_{AW} at 492 nm (in orange).

Figure 8: P_{AW} peptide prevents HIV-1 RT dissociation. (A) P_{AW} associated protection of RT from the acetonitrile dissociation as monitored by size exclusion chromatography. First, HIV-1 RT (8.7 µM) was incubated in the presence (red line) or absence (blue line) of fluorescently labelled P_{AW} (100 µM) then dissociated by 17% acetonitrile for 30 min at room temperature and applied onto a size exclusion chromatography. (B) Kinetics of RT dissociation induced by acetonitrile. RT (0.5 µM) was dissociated in the presence of 0.8 µM bis-ANS, by adding 10 % acetonitrile in the absence (blue line) or presence of 5 µM P_{AW} (red line). The kinetics of dissociation were monitored by following the fluorescence resonance energy transfer between tryptophan of RT and Bis-ANS. Tryptophan excitation was performed at 290 nm and the increase of bis-ANS fluorescence emission at 490 nm was detected through a 420 nm cut-off filter. Data acquisition and analysis were performed using KinetAsyst 3 software (Hi-Tech Scientific, Salisbury, England-UK) and traces were fitted according to a single exponential equation.

Table 1: Sequences and inhibition of polymerase activity of HIV-1 RT by Pep-A derived peptides.

Peptides	Sequences	Ki (µM) [a]
PepA	RGTKALTEVIPLTEEAEC	35± 5
P1	GTKALTEVIPLTEEAEC	7.5± 2.3
P2	ATKALTEVIPLTEEAEC	28± 11
P3	GAKALTEVIPLTEEAEC	10.3± 2.1
P4	GTAALTEVIPLTEEAEC	15± 2.9
P5	GTKGLTEVIPLTEEAEC	20± 3.7
P6	GTKAATEVIPLTEEAEC	5.7± 2.3
P7	GTKALAEVIPLTEEAEC	13.5± 2.1
P8	GTKALTAVIPLTEEAEC	57± 19
P9	GTKALTEAIPLTEEAEC	15± 7.3
P10	GTKALTEVAPLTEEAEC	7.3± 2.9
P11	GTKALTEVIALTEEAEC	7± 1.4
P12	GTKALTEVIPATEEAEC	22± 3
P13	GTKALTEVIPLAEEAEC	10.2± 2.5
P14	GTKALTEVIPLTAEAEC	14± 3
P15	GTKALTEVIPLTEAAEC	14± 2.2
$P_{scramble}$	GAKTETLVIPETELEAC	61 ± 12
P_{AW}	GTKWLTEWIPLTAEAEC	0.7± 0.2
P_{AW}-*FITC*	GTKWLTEWIPLTAEAEC-*FITC*	2.7 ± 0.7

[a.] RT polymerase activity was measured as described in the Materials and Methods. The inhibition constants Ki were calculated from Dixon plots and reported data correspond to the mean of three separate experiments.

Table 2: Antiviral activity of Pep-A and P_{AW}-derived peptides

Peptides	EC_{50} (nM) [a]	SI [b]
P1/Pep-1	78.2	>ND
P6/Pep-1	170	> 3
P8/Pep-1	290	> 3
P10/Pep-1	140	ND
P_{AW}	> 1000	ND
P_{AW}/Pep-1	1.8	> 550
P18/Pep-1	>1000	ND
P24/Pep-1	2.3	> 1200
P26/Pep-1	>1000	ND
P27	> 1000	ND
P27/Pep-1	< 0.32	> 3100

a. anti-HIV activity was evaluated on PHA-P-activated PBMC infected with HIV-1-LAI strain. EC_{50} values correspond to the 50% effective peptide dose

b. Selectivity index, which corresponds to the ratio between EC_{50} and the cytotoxic concentration (CC_{50}) inducing 50% death of uninfected PBMCs

ND: value not determined

Table 3 : P_{AW}-derived peptide sequences and Inhibition of polymerase activity of HIV-1 RT.

Peptides	Sequences	Ki(µM) [a]
P_{AW}	GTKWLTEWIPLTAEAEC	0.7± 0.2
P16	GTKWLTEVWPLC	14± 4
P17	GTKAWTEVWPLC	35± 11
P18	GTKALTEVIPLTC	53± 12
P19	GTKAATEVIPLTC	49± 9
P24	GTKWLTEWIPLC	0.7± 0.05
P26	KWLTEWIPLTAEAEC	1.8± 0.7
P27	GTKWLTEWIPLTAEC	0.05± 0.01
P28	GTKWATEWAPLTAEAEC	2± 0.6
P29	KWLTEWIPLTAEC	1± 0.4

[a.] RT polymerase activity was measured as described in the Materials and Methods. The inhibition constants Ki were calculated from Dixon plots and reported data correspond to the mean of three separate experiments.

Figure 1

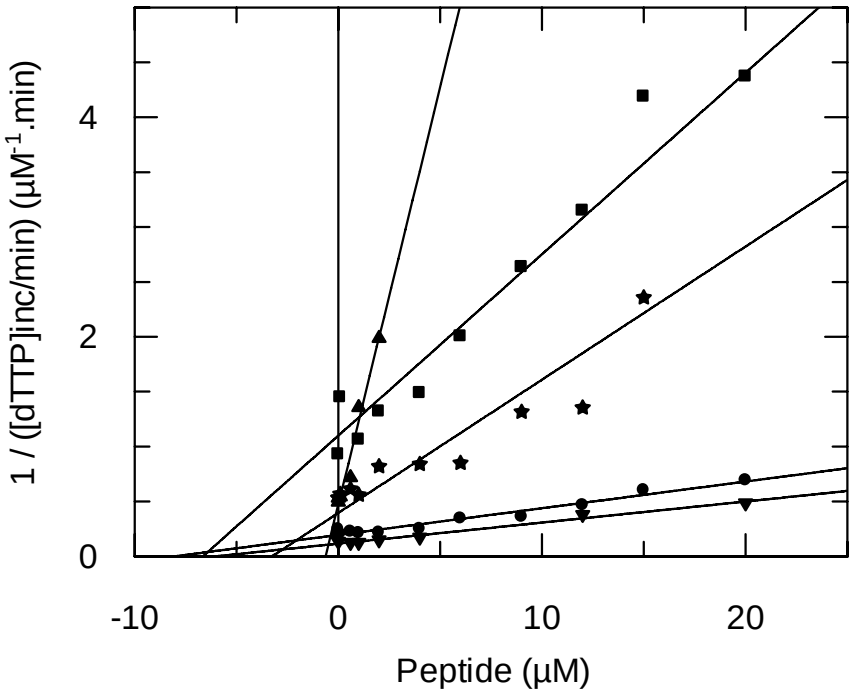

Figure 2

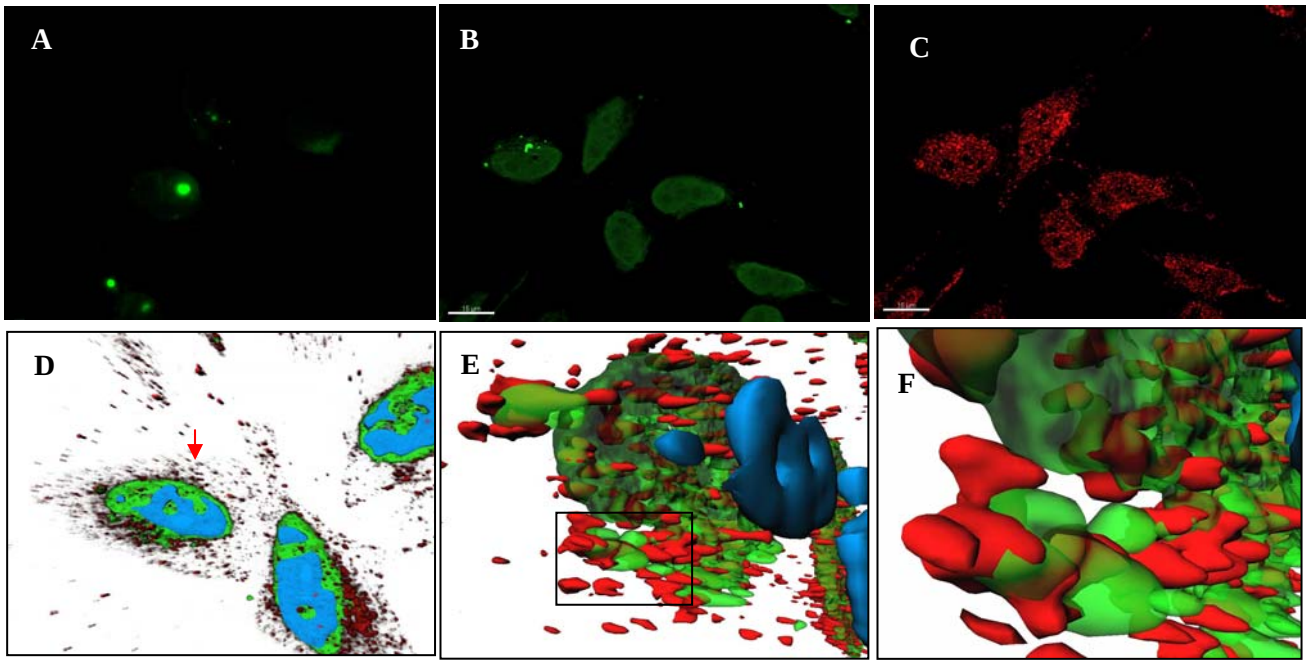

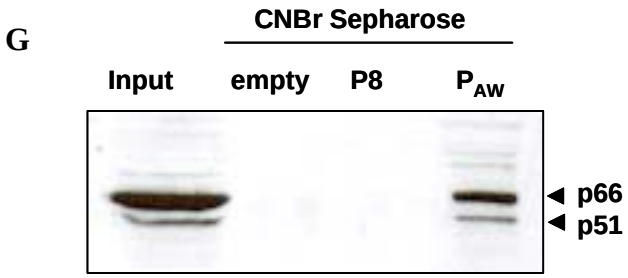

Figure 3

A

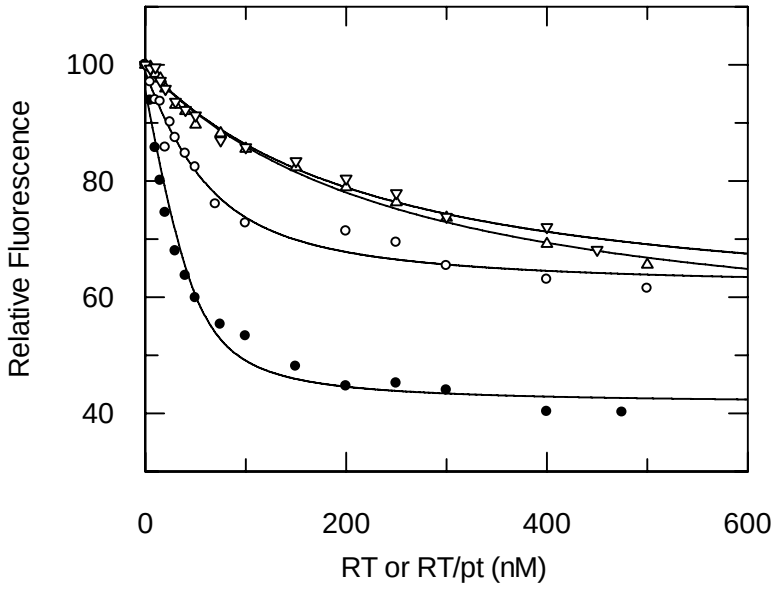
Relative Fluorescence
100
80
60
40
0
200
400
600
RT or RT/pt (nM)

B

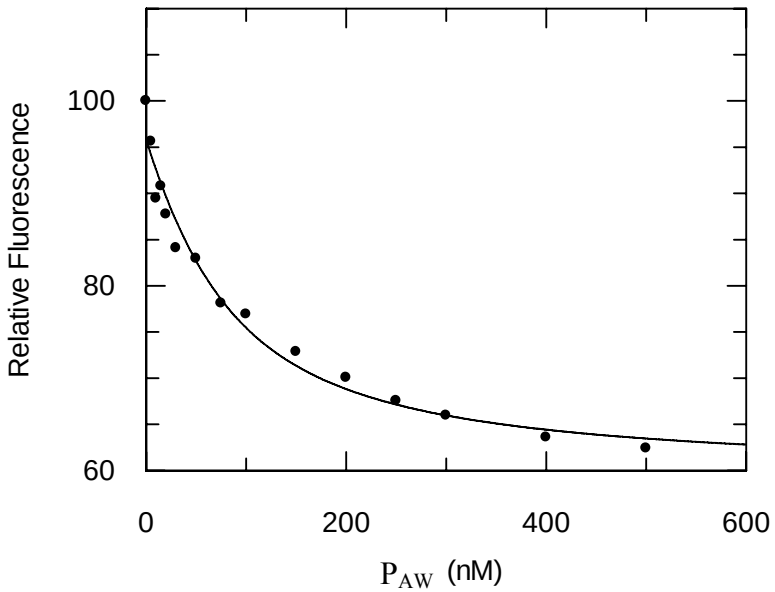
Relative Fluorescence
100
80
60
0
200
400
600
P_{AW} (nM)

Figure 4

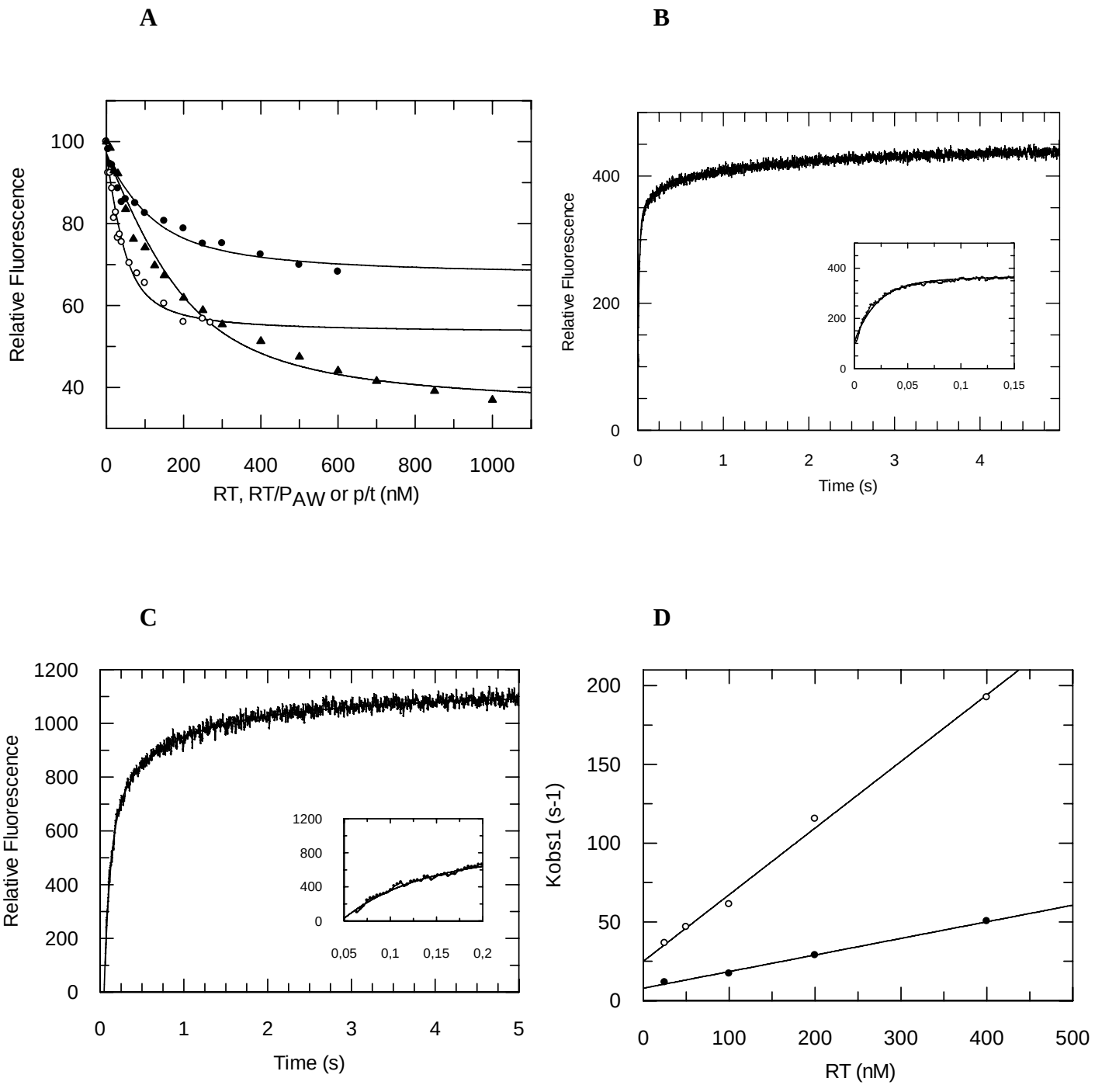
A
B
C
D
Relative Fluorescence
RT, RT/P_AW or p/t (nM)
Time (s)
Kobs1 (s-1)
RT (nM)

Figure 5

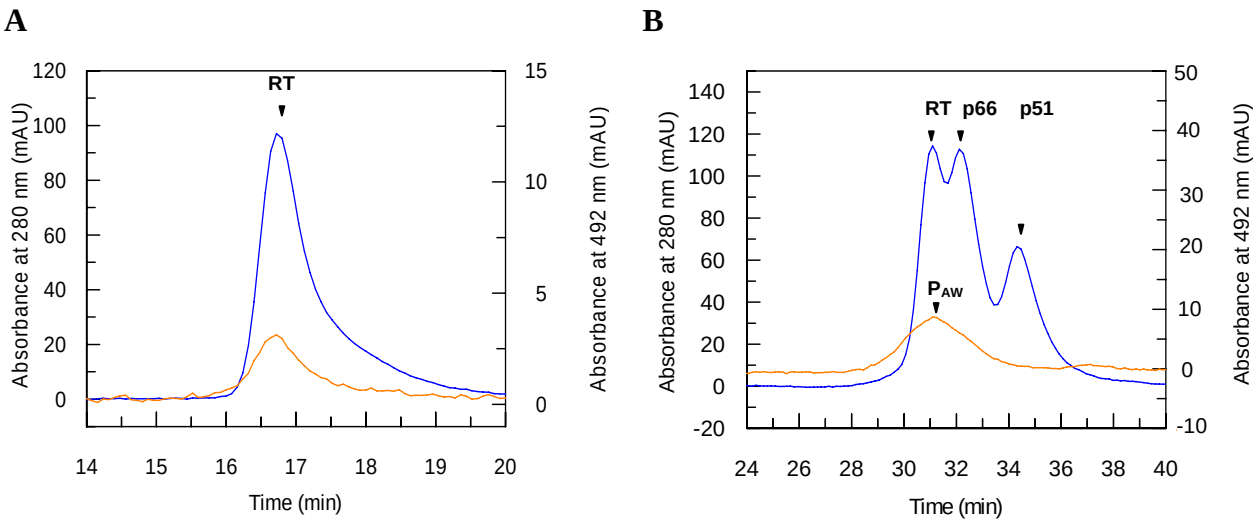
A
RT
Absorbance at 280 nm (mAU)
Absorbance at 492 nm (mAU)
Time (min)
B
RT p66 p51
PAW
Absorbance at 280 nm (mAU)
Absorbance at 492 nm (mAU)
Time (min)

Figure 6

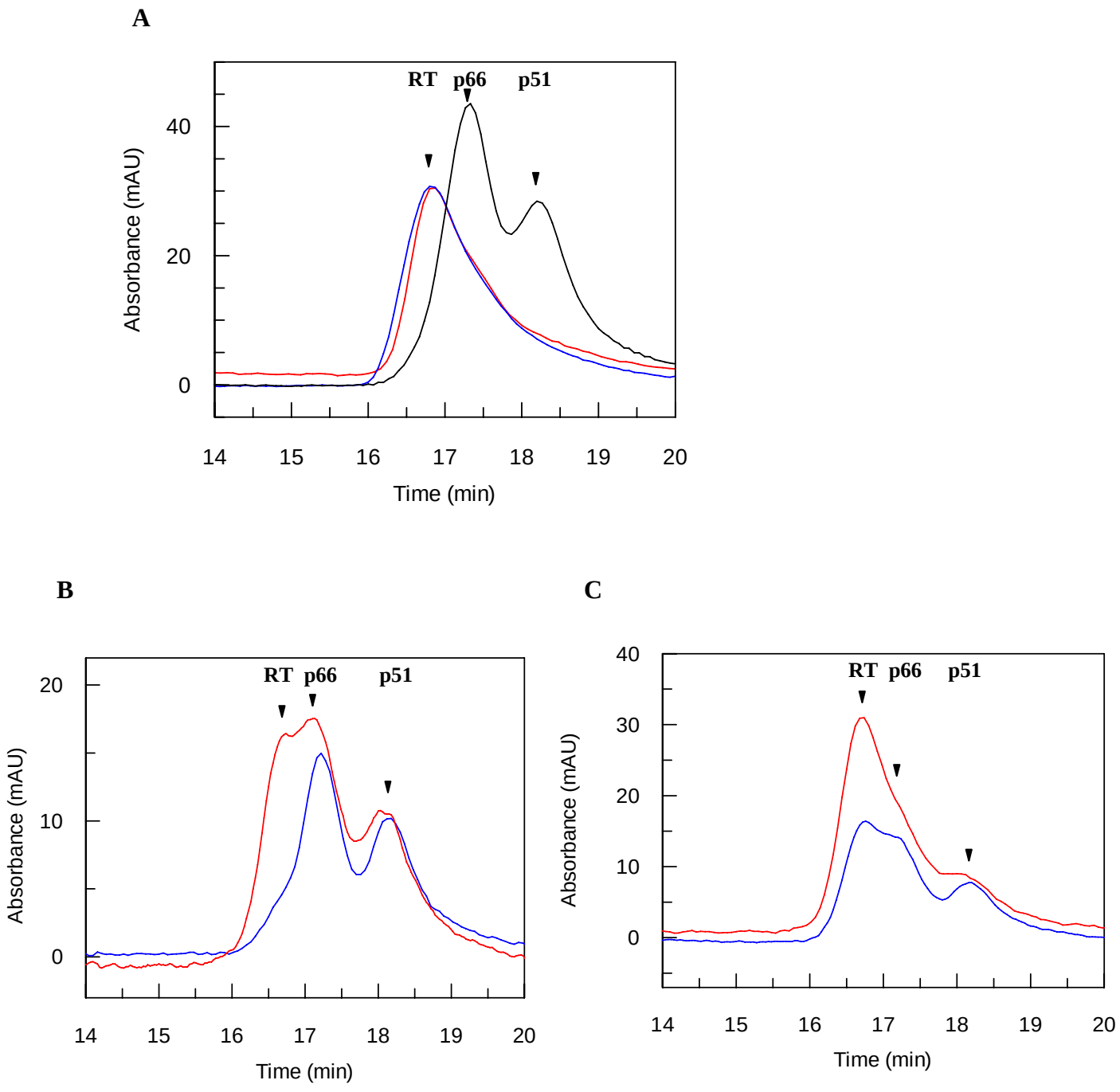
A
RT
p66
p51
Absorbance (mAU)
Time (min)
B
RT
p66
p51
Absorbance (mAU)
Time (min)
C
RT
p66
p51
Absorbance (mAU)
Time (min)

Figure 7

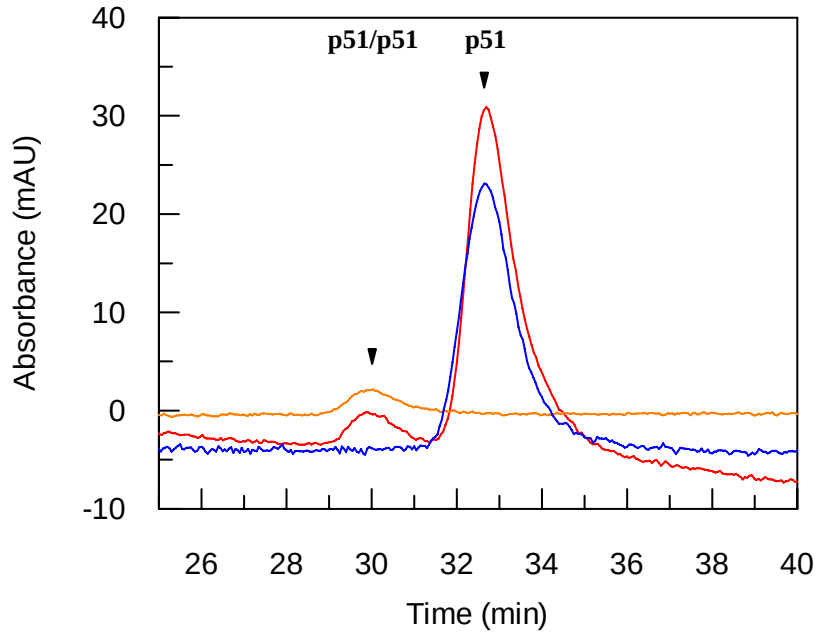
p51/p51
p51
Absorbance (mAU)
40
30
20
10
0
-10
26
28
30
32
34
36
38
40
Time (min)

Figure 8

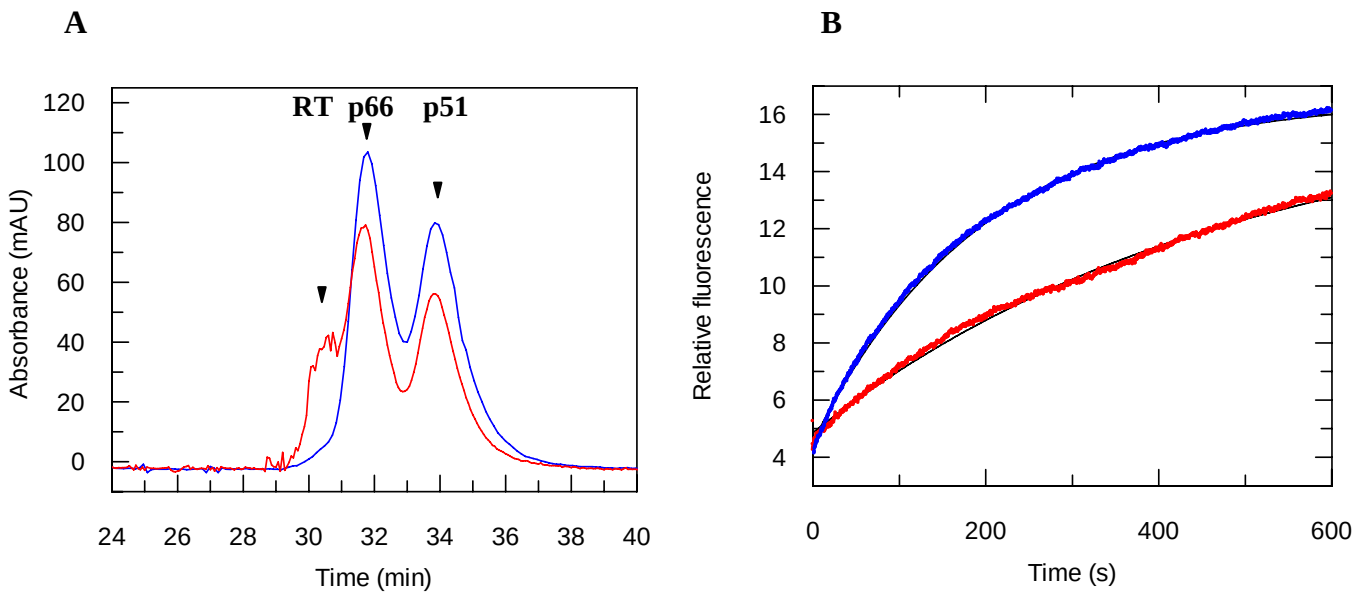
A
RT
p66
p51
Absorbance (mAU)
120
100
80
60
40
20
0
24
26
28
30
32
34
36
38
40
Time (min)
B
Relative fluorescence
16
14
12
10
8
6
4
0
200
400
600
Time (s)